Food Research International 111 (2018) 111–119

Contents lists available at ScienceDirect

Food Research International

journal homepage: www.elsevier.com/locate/foodres

Quantitative evaluation of the risk of *Vibrio parahaemolyticus* through consumption of raw oysters (*Crassostrea corteziensis*) in Tepic, Mexico, under the RCP2.6 and RCP8.5 climate scenarios at different time horizons

Mario A. Ortiz-Jiménez

Departamento de Ciencias Básicas, Instituto Tecnológico de Tepic, Av. Tecnológico # 2595, Col. Lagos del Country, Tepic, Nayarit C.P. 63175, Mexico

ARTICLE INFO

Keywords:
Risk assessment
Postharvest time
Mitigation
Simulation
NOM-242-SSA1-2009
Climate change
Pleasure oyster
Gastroenteritis

ABSTRACT

Little is known about the impacts on public health of pathogenic *Vibrio parahaemolyticus* under different climatic scenarios and future time horizons. A simulation model was developed based on the Monte Carlo method to evaluate the effect of the factors that contribute to the growth of *Vibrio parahaemolyticus* from its estuary environment to its end consumption in different seasons, climatic scenarios and time horizons. The factors that most contribute to risk of gastroenteritis were postharvest time, season, time horizon and the climate scenario. The predicted risk increases with postharvest time, nearing a plateau of 0.010 after 36 h when risk is 5 times higher than that at 0 h postharvest. There are significant differences in risk among the seasons: in summer the risk is almost double that in winter, and in fall it is higher than in spring. The time horizon significantly affects the predicted risk, increasing 1.12 times from 2020 to 2100. There is significant evidence that the climate scenario affects predicted risk per serving: risk in the RCP8.5 scenario intensifies to 11 times that in the RCP2.6 scenario. Moreover, the effectiveness of mitigation measures to reduce the level of *Vibrio parahaemolyticus* in raw oysters was evaluated with respect to the official Mexican norm NOM-242-SSA1-2009. Using as reference the risk of becoming ill in summer from consuming recently harvested oysters with no mitigation in any climate scenario and time horizon, immediate refrigeration would reduce risk of disease by 37%. In contrast, depuration would reduce it by 94%, and freezing, heat treatment and thermal shock would reduce it by almost 100%.

1. Introduction

Anthropogenic emissions of greenhouse gases have accumulated in the atmosphere during the last 50 years, causing global warming and subsequent climate change. It is expected that this variability in the planet's climate pattern will exacerbate existing health problems (IPCC, 2014) and increase incidence of infections transmitted by water and food (McMichael & Lindgren, 2011; Smith et al., 2015). Particularly, diseases caused by *Vibrio* species have a disturbing upward trend worldwide (Burge et al., 2014; Vezzulli, Colwell, & Pruzzo, 2013). Warming of littorals in middle and high latitudes has been associated with outbreaks of *V. parahaemolyticus* from consuming raw seafood, such as those reported in Alaska, Spain and India (Martinez-Urtaza et al., 2016; McLaughlin et al., 2005; Pazhani et al., 2014). Today, *V. parahaemolyticus* is the bacterium that prevails in food poisoning associated with consumption of raw seafood in many Asian countries (Alam, Tomochika, Miyoshi, & Shinoda, 2002), and it is the main microorganism identified as the cause of human gastroenteritis in the United States (Newton, Kendall, Vugia, Henao, & Mahon, 2012). The strains associated with the disease have one or two hemolysin genes that code the thermostable direct hemolysin (*tdh*), which is responsible for Kanagawa hemolysis and the hemolysin related to *tdh* (*trh*) (Bej, 1999).

Quantitative microbial risk assessment (QMRA) is a methodology established to evaluate public health risks associated with pathogenic organisms (Haas, Rose, & Gerba, 2014) and instituted to establish policies and regulations to reduce the load of food-borne diseases (Gkogka, Reij, Gorris, & Zwietering, 2013). Several QMRA studies have reported *V. parahaemolyticus* infection caused by consumption of raw seafood, among which black tiger shrimp in Malaysia (Sani, Ariyawansa, Babji, & Hashim, 2013), bloody clams in Thailand (Yamamoto et al., 2008), horse mackerel in Japan (Iwahori et al., 2010) and raw oysters in the U.S. (FDA, 2005), Brasil (Sobrinho, Destro, Franco, & Landgraf, 2010) and Taiwan (Yen-Shan Huang, Hwang, Huang, Wu, & Hsiao, 2017) are outstanding. In the measure that the planet warms, there is a possibility of an increase in infections caused by *V. parahaemolyticus* associated with consuming raw seafood. The importance of this study lies in the estimation of risk of disease caused by *V. parahaemolyticus* through consumption of raw oysters under

E-mail address: ojimez@gmail.com.

https://doi.org/10.1016/j.foodres.2018.05.012
Received 2 February 2018; Received in revised form 19 April 2018; Accepted 7 May 2018
Available online 09 May 2018
0963-9969/ © 2018 Elsevier Ltd. All rights reserved.

different combinations of seasons, climate scenarios, postharvest times and time horizons. The results of this study could help risk managers and oyster processors to develop control measures to reduce risk of *V. parahaemolyticus* infection from consuming raw oysters.

One of the greatest challenges of the health sector is to evaluate the impact of climate change on risk of contracting infectious diseases caused by *Vibrio*. Using data available in the literature (FDA, 2005), we developed a model to predict the impact on public health of pathogenic *V. parahaemolyticus* present in raw oysters cultivated in Boca de Camichín and consumed in the city of Tepic, Mexico, under different combinations of seasons, climate scenarios, postharvest times and time horizons. The objective was to develop a Monte Carlo simulation model using the software @Risk, version 7.5.2 (Palisade Corportarion, 2017), a complement of Excel risk analysis (Microsoft, 2017), to evaluate the effect of factors that contribute to growth of *V. parahaemolyticus* from the estuary environment to its final consumption under different environmental conditions. Moreover, we evaluated the different mitigation measures and their effectiveness in reducing levels of *V. parahaemolyticus* in raw oysters relative to the requirements established by the official Mexican norm NOM-242-SSA1 (2009) under different combinations of climate scenarios and time horizons.

Nayarit is the largest producer of pleasure oysters (*Crassostrea corteziensis*) in the Mexican Pacific region, with a production of 3250 t of the mollusk in 2016 (CONAPESCA, 2017). However, its commercialization is limited to the domestic market because the water where it is farmed does not comply with approved area criteria established by NOM-242-SSA1 (2009). Boca de Camichín, located at the mouth of the San Pedro River, concentrates 70 or 80% of the state's oyster production. Tepic, the state capital of Nayarit, is one of the main consumers of oysters. It is located 94 km southeast of Boca de Camichín, and in 2010 had 332,863 inhabitants (INEGI, 2010) with an annual per capita oyster consumption of 0.41 kg (INEGI, 2013).

2. Material and methods

2.1. Simulation of air and water temperatures of the Boca de Camichín estuary

We obtained the historical records of daily temperatures available from the Guadalupe Victoria weather station, located 19 km southeast of Boca de Camichín (INIFAP, 2017). Table 1 summarizes the mean daily temperatures (μ_μ), standard deviations of the daily temperatures (σ_μ), means of the standard deviations of daily temperatures (μ_σ), the standard deviations of the standard deviations of daily temperatures (σ_σ), and the correlation coefficients of daily temperatures and standard deviations of daily temperatures (ρ) for each season of the year.

We calculated the variance-covariance matrix and the respective square root:

$$A = \begin{bmatrix} E_{11} = \mu_\sigma, & E_{12} = \rho\sqrt{\mu_\sigma \sigma_\sigma} \\ E_{21} = \rho\sqrt{\mu_\sigma \sigma_\sigma}, & E_{22} = \sigma_\sigma \end{bmatrix} \quad (1)$$

$$B = \begin{bmatrix} R_{11} = \sqrt{\mu_\sigma}, & R_{12} = 0 \\ R_{21} = \rho\sqrt{\sigma_\sigma}, & R_{22} = \sqrt{\rho_\sigma}(1-\rho^2)/\sqrt{1-\rho^2\mu_\sigma} \end{bmatrix} \quad (2)$$

Randomly, the mean air temperature (μ_{Tair}) and the standard deviation of that temperature (σ_{Tair}) were generated for each of the stations using the following expressions:

$$\mu_{Tair} = \mu_\mu + R_{11}z_1 + R_{12}z_2 \quad (3)$$

$$\sigma_{Tair} = \mu_{\sigma^2} + R_{21}z_1 + R_{22}z_2 \quad (4)$$

where $z_i \sim RiskNormal(0,1)$ for $i = 1, 2$.

The following random variable was used to simulate air temperature of Boca de Camichín for each season of the year:

$$T_{air} \sim RiskNormal(\mu_{Tair}, \sigma_{Tair}) \quad (5)$$

Table 2 shows the fitted regression models of daily observed water temperature in Boca de Camichín (T_w) in function of the observed daily air temperature at Guadalupe Victoria (T_{air}).

Table 1
Daily temperature statistics of Guadalupe Victoria (°C).

Season	μ_μ	σ_μ	μ_σ	σ_σ	ρ
Spring	24.8956	2.4005	4.9330	0.2655	−0.0851
Summer	28.1800	1.4909	1.3751	0.0848	0.2333
Fall	24.9369	2.2993	2.3592	0.2465	−0.2841
Winter	19.9949	2.6493	2.8353	0.3107	−0.1733

Table 2
Relationship between observed water and air temperatures.

Season	Regression model	R^2
Spring	$T_w = 8.232 * exp(0.0453 * T_{air})$	0.987
Summer	$T_w = 25.615 * exp(0.0067 * T_{air})$	0.999
Fall	$T_w = 18.711 * Ln(T_{air}) - 31.594$	0.993
Winter	$T_w = 12.478 * exp(0.0336 * T_{air})$	0.994

2.2. Simulation of climate scenarios

The Fifth IPCC Report defined four future scenarios of greenhouse gas emissions denominated Representative Concentration Trajectories (RCP): a scenario with a minimum of greenhouse gas emissions (RCP2.6), two scenarios of stabilization (RCP4.5 and RCP6.0), and one scenario with a very high level of greenhouse gas emissions (RCP8.5). Fig. 1 shows the projections of expected global surface temperature changes for scenarios RCP2.6 and RCP8.5 in the time horizons 2020, 2060 and 2100 (IPCC, 2014).

2.3. Simulation model

This quantitative risk evaluation is based on a probabilistic simulation model developed by the FDA (2005) for the current climate scenario and was modified to include the effects of climate scenarios and time horizons at different postharvest times. Each run of the model represented a serving of oysters whose *V. parahaemolyticus* level in the estuary environment is a function of water temperature. The rate of *V. parahaemolyticus* growth during harvest and postharvest is in function of postharvest time, air temperature and water activity. We simulated weight of the flesh of each oyster, number of oysters per serving and the

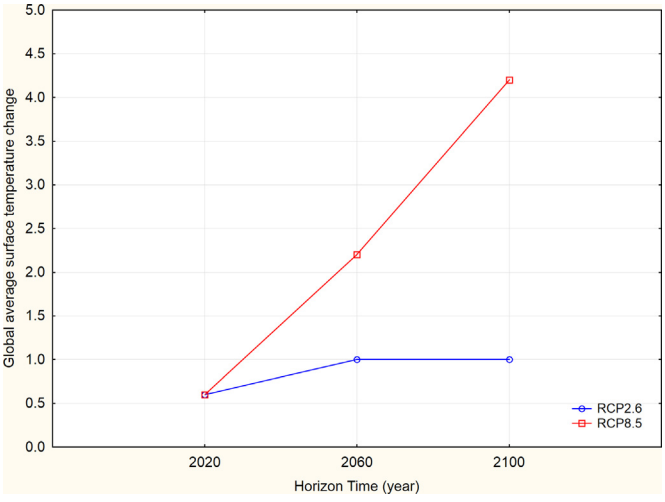

Fig. 1. Average global surface temperature change.

level pathogenic and total of *V. parahaemolyticus*, per serving. We used a quantitative relationship to predict the risk of gastroenteritis in function of ingesting different doses of pathogenic *V. parahaemolyticus* per serving, including subpopulations of healthy consumers and of individuals with pre-existing medical conditions. We calculated pathogenic and total levels of *V. parahaemolyticus* per gram of consumed oyster and the risk of becoming ill in two climate scenarios (RCP2.6 and RCP8.5), three time horizons (2020, 2060 and 2100), four postharvest times (0, 12, 24 and 48 h) and six mitigation strategies (no mitigation, freezing, thermal shock, heat treatment, immediate refrigeration and depuration). To validate the model, the pathogenic and total levels of *V. parahaemolyticus* predicted by the model were compared against the data reported by Mendoza-Juárez (2015) for raw oysters acquired in Tepic and cultivated in Boca de Camichín.

The model was based on the following assumptions: 1) the oysters that make up one serving have the same weight and the same postharvest time; 2) the growth rates of pathogenic and total *V. parahaemolyticus* are the same; 3) the maximum density of total *V. parahaemolyticus* per gram of oyster is 10^6 MPN at any temperature; 4) the fraction of pathogenic *V. parahaemolyticus* of the total is considered constant and equal to 0.0031 (Mendoza-Juárez, 2015) and is independent of water and air temperatures; 5) the consumption patterns of healthy consumers and those with pre-existing medical condition are equal and do not change over time; 6) the predicted risk corresponds to oysters cultivated in Boca de Camichín and consumed in Tepic; 7) the risks of disease were calculated for a 154 g average serving of oysters; and 8) all the strategies of mitigation are applied immediately after oyster harvest.

Simulations of the model were done in @Risk version 7.5.2 (Palisade Corportarion, 2017) using the Monte Carlo method. Each combination of season-climate scenario-time horizon-postharvest time was replicated five times, each replication formed by the averages of predicted risk and levels of pathogenic and total *V. parahaemolyticus* of 1000 simulation runs.

2.4. Data analysis

Because the response variables (predicted risk and total and pathogenic levels of *V. parahaemolyticus*) did not behave normally, nonparametric statistical techniques were used. The statistical analyses were conducted using the software STATISTICA version 10 developed by StatSoft (2011) for Windows. To compare climate scenarios, the Mann-Whitney *U* test was used, and to compare the time horizons, postharvest times and seasons, the Kruskall-Wallis tests were used. A post-hoc comparison was then made of the mean ranks of all the pairs of groups (Siegel & Castellan, 1988) by calculating the z' values for each comparison of the u and v groups:

$$z'_{u,v} = \frac{|\overline{R}_u - \overline{R}_v|}{\sqrt{\frac{N(N+1)}{12}\left(\frac{1}{n_u} + \frac{1}{n_v}\right)}} \tag{6}$$

where $\overline{R}_u$ and $\overline{R}_v$ denotes the average ranks for the two groups, n_u and n_v are the number of observations in the two groups (u and v), and $N = n_u + n_v$.

The p-value (two-sided significance levels with a Bonferroni adjustment) associated with each comparison, were computed as:

$$p = 2k(k-1)[1 - P(Z < z'_{u,v})] \tag{7}$$

where k stands for the total number of groups in the comparison, and the p-values were calculated using the *Nonparametrics* module of STATISTICA (StatSoft, 2011).

We constructed graphs of the combinations season-climate scenario-time horizon-postharvest time against the response variables to visualize interactions of interest.

3. Calculations

We used a Tobit regression probabilistic model (Cameron & Windmeijer, 1996; Cameron & Windmeijer, 1997) to calculate the growth of total *V. parahaemolyticus* per gram of oyster in the estuary environment in function of water temperature (T_w) using the parameter values recommended by the Washington State Department of Health (2000, 2001).

$$LogV_{t,en} = \begin{cases} \alpha + \beta * T_w + RiskNormal(0,\sigma) & si\ LogV_{t,en} < 6 \\ 6 & si\ LogV_{t,en} \geq 6 \end{cases} \tag{8}$$

where $\alpha \sim RiskPert(-5.77, -4.32, -2.88)$, $\beta \sim RiskPert(0.16,0.2,0.32)$ and $\sigma \sim RiskPert(0.61,0.78,0.99)$.

Mendoza-Juárez (2015) reported a pathogenic fraction of *V. parahaemolyticus* of 0.003 in oysters cultivated in Boca de Camichín. Therefore, the maximum level of pathogenic *V. parahaemolyticus* per gram of oyster in the estuary environment was calculated with the expression:

$$MLogV_{p,en} = 6 + Log(0.0031) \tag{9}$$

The level of pathogenic *V. parahaemolyticus*/g in the estuary environment was calculated with the expression:

$$LogV_{p,en} = \begin{cases} Log(0.0031) + LogV_{t,en} & si\ Log(0.0031) + LogV_{t,en} < MLogV_{p,en} \\ MLogV_{p,en} & si\ Log(0.0031) + LogV_{t,en} \geq MLogV_{p,en} \end{cases} \tag{10}$$

Table 3 presents the probabilistic distributions of the different times used in the model.

Postharvest time is the sum of transportation time from Boca de Camichín to Tepic and wait time in Tepic until end consumption. The Miles, Ross, Olley, and McMeekin (1997) model was used to calculate the square root of the maximum growth rate in function of air temperature T_{air} (°K) and water activity (a_w):

$$\sqrt{\mu_m} = \frac{0.356(T_{air} - 278.5)\{[1 - exp(0.34(T_{air} - 319.6))]\sqrt{(a_w - 0.921)[1 - exp(263.64(a_w - 0.998))]}\}}{\theta\sqrt{Ln(10)}} \tag{11}$$

where $\theta \sim RiskTriang(3,4,5)$ is an axenic factor recommended by Gooch, DePaola, Bowers, and Marshall (2002). The maximum growth rate of total *V. parahaemolyticus* (in log10/g*min) was calculated with the expression:

$$\mu_m = \begin{cases} \sqrt{\mu_m} * \sqrt{\mu_m}, & si\ \sqrt{\mu_m} > 0 \\ 0, & si\ \sqrt{\mu_m} \leq 0 \end{cases} \tag{12}$$

Growth of total *V. parahaemolyticus*/g of oyster during harvest was calculated with the expression:

$$GLogV_{t,h} = Min[6 - LogV_{t,en}, \mu_n \times 60 \times RiskPert(0.5,6,7)] \tag{13}$$

where the minimum time the oysters were out of the water was half an hour, the most probable time out of the water was 6 h and the maximum time out of water was 7 h.

Table 3
Probabilistic distributions at different times.

Time (hours)	Probabilistic distribution
Oyster harvest	*RiskPert*(0.5,6,7)
Transportation to Tepic	3 + *RiskPert*(2,3,4)
Wait time at the point of consumption	*RiskTriang*(1,8,72)

$$LogV_{t,h} = \begin{cases} LogV_{t,en} + GLogV_{t,h} \; si \; LogV_{t,en} + GLogV_{t,h} < 6 \\ 6, \qquad\qquad si \;\; LogV_{t,env} + GLogV_{t,h} \geq 6 \end{cases} \quad (14)$$

The level of total *V. parahaemolyticus*/g oyster up to consumption was calculated with the expression:

$$LogV_{t,ph} = Min(6 - LogV_{t,h}, \mu_n \times t_{ph} \times 60) \quad (15)$$

where t_{ph} is postharvest time in hours.

The accumulated level of total *V. parahaemolyticus*/g from the estuary environment to consumption was calculated with the expression:

$$LogV_{t,ac} = \begin{cases} LogV_{t,en} + GLogV_{t,h} + LogV_{t,ph} \;\; si \; LogV_{t,en} + GLogV_{t,h} \\ \qquad + LogV_{t,ph} < 6 \\ 6, \qquad\qquad\qquad\qquad\qquad\qquad si \;\; LogV_{t,en} + GLogV_{t,h} \\ \qquad\qquad\qquad + LogV_{t,ph} \geq 6 \end{cases} \quad (16)$$

The accumulated count of pathogenic *V. parahaemolyticus*/g from the estuary environment to consumption was calculated with the expression:

$$LogV_{p,ac} = \begin{cases} LogV_{t,ac} + Log(0.0031), \quad si \; LogV_{t,ac} \\ \qquad + Log(0.0031) < MLogV_{p,en} \\ MLogV_{p,en} \qquad\qquad si \; LogV_{t,ac} + Log(0.0031) \\ \qquad \geq MLogV_{p,en} \end{cases} \quad (17)$$

The number of oysters per serving (n_{ser}) was generated randomly with a discrete distribution that assigns 80% probability to consumers that order a dozen oysters and 10% to those that order half or two dozen:

$$n_{ser} \sim RiskDiscrete(\{6, 12, 24\}, \{0.1, 0.8, 0.10\}) \quad (18)$$

The weight of each oyster was fit to a *RiskLognorm*2(2.126984,0.98961) distribution. We considered that 90% of the weight of shelled oysters is flesh and the minimum and maximum consumption of flesh per serving was 100 and 400 g, respectively. Weight of oyster flesh per serving was calculated with the expression:

$$W_{ser} = Max[100, Min(0.9 \times RiskLognorm2(2.126984, 0.98961) \times n_{ser}, 400)] \quad (19)$$

The level of pathogenic *V. parahaemolyticus* consumed per serving was calculated with the expression:

$$V_{p,ser} = (10^{LogV_{p,ac}}) \times W_{ser} \quad (20)$$

which was rounded off using a function of Poisson:

$$RV_{p,ser} = RiskPoisson(V_{p,ser}) \quad (21)$$

The Beta-Poisson dose response model was used to calculate the risk of becoming ill with gastroenteritis in function of the dose of pathogenic *V. parahaemolyticus* consumed (FAO/WHO, 2003; FDA, 2005):

$$P(gastroenteritis \mid dose) = 1 - \left(1 + \frac{RVp_{p,ser}}{27.1 \times \beta}\right)^{-\alpha} \quad (22)$$

where α and β are maximum likelihood parameters that depend on the virulence characteristics of the strain, the food matrix and the susceptibility or immune state of the host. Fig. 2 shows the discrete probabilistic distribution of the 21 different Beta-Poisson models, each associated with a pair of values (α, β) (FDA, 2005).

For the case of immediate refrigeration, the harvested oysters are placed in chipped ice in the boat, where it takes an hour to reach a temperature at which there is no growth (Schwarz, 2003). Growth of total *V. parahaemolyticus* in these conditions is equivalent to half the growth at ambient temperature for an hour:

$$GLogV_{t,ice} = (\mu_n \times 1 \times 60)/2 \quad (23)$$

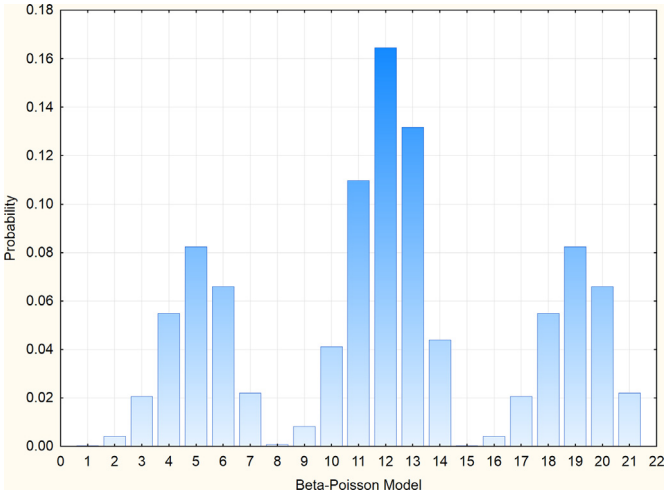

Fig. 2. Probabilities of occurrence of the 21 Beta-Poisson models.

where μ_n was obtained from expression (12).

The level of total *V. parahaemolyticus* after cooling with ice was calculated with the following expression:

$$LogV_{t,ice} = \begin{cases} LogV_{t,en} + GLogV_{t,ice} \; si \; LogV_{t,en} + GLogV_{t,ice} < 6 \\ 6, \qquad\qquad si \;\; LogV_{t,en} + GLogV_{t,ice} \geq 6 \end{cases} \quad (24)$$

The level of total *V. parahaemolyticus* after immediate refrigeration up to a certain time postharvest inside a refrigerator was calculated with the expression (FAO/WHO, 2011):

$$LogV_{t,die-off} = LogV_{t,ice} - 0.0027(t_{ph} - 1) \quad (25)$$

Also, the level of total *V. parahaemolyticus* after depuration was calculated with the following equation:

$$LogV_{t,dep} = LogV_{t,h} - RiskUniform(0, 2) \quad (26)$$

4. Results and discussion

4.1. Risk assessment model

The three Beta-Poisson models (Alam et al., 2002; FDA, 2005; Martinez-Urtaza et al., 2016) of Fig. 3 represent the response of consumer subpopulations that are little, intermediately and highly susceptible to the disease, respectively, when ingesting a given dose of pathogenic *V. parahaemolyticus*. For the case of a highly susceptible subpopulation, there is a marked difference between the response to a serving of 300 g of recently harvested oysters, served in Boca de Camichín in an RCP2.6 scenario in the summer of 2020, and another serving of 300 g of oysters with no mitigation and 12 h postharvest time served in Tepic in the summer with an RCP8.5 scenario in 2100. In the first case, the likelihood of becoming sick is 10% and in the second, the probability increases 7 times, > 70%, while the probability that the subpopulation that is little or intermediately susceptible becomes ill is practically zero.

A Mann-Whitney *U* test found significant evidence that the climate scenario affects predicted risk per serving: risk in the RCP8.5 scenario intensifies to 11 times that in the RCP2.6 scenario ($p < 0.001$). Based on the prediction model, we foresee that climate temperatures trends match future scenarios of risk of *Vibrio* infection (Baker-Austin et al., 2013). Because no consensus has been reached among developed countries to limit greenhouse gas emissions into the atmosphere, an RCP8.5 climate scenario is possible in the coming decades, increasing eleven-fold the possibilities of *V. parahaemolyticus* infection among consumers of raw oysters in Tepic.

A Kruskall-Wallis test found that the time horizon significantly

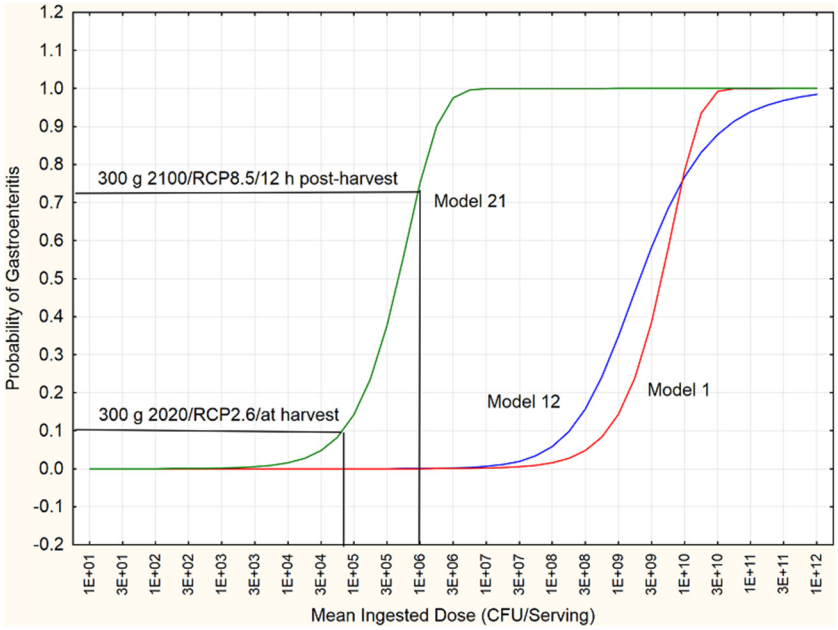

Fig. 3. Beta-Poisson dose-response (FDA, 2005).

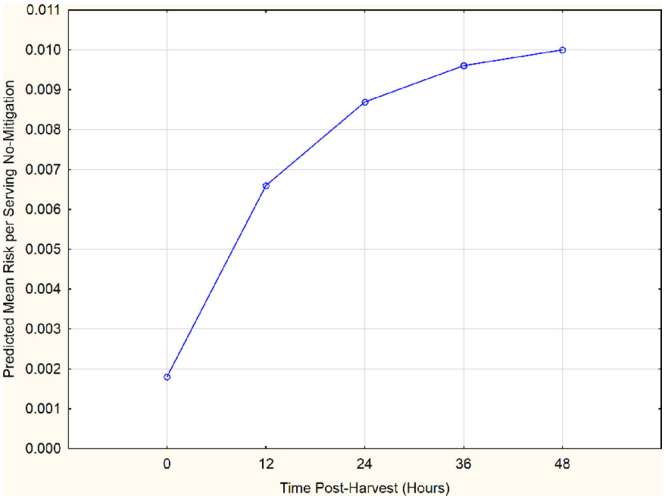

Fig. 4. Effect of postharvest time.

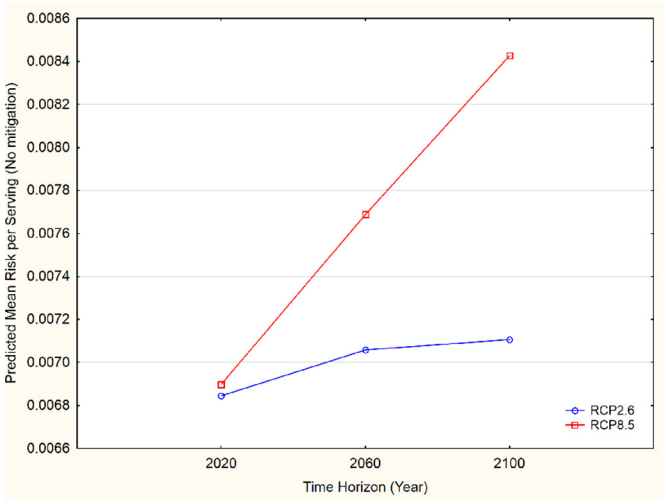

Fig. 5. Interaction time horizon-climate scenario.

affects the predicted risk, increasing 1.12 times the risk from 2020 to 2100 ($p < 0.001$). Another Kruskall-Wallis test revealed significant differences in risks among the seasons: in summer the risk is almost double that in winter, and in fall it is higher than in spring ($p < 0.001$). The highest densities of *V. parahaemolyticus* are associated with high summer temperatures (DePaola, Nordstrom, Bowers, Wells, & Cook, 2003), and it is known that risk of *Vibrio*-related gastroenteritis increases when seafood is consumed in summer (ANSES, 2012). Fig. 4 shows how predicted risk increases with postharvest time, nearing a plateau of 0.010 after 36 h when risk is 5 times higher than that at 0 h postharvest ($p < 0.001$). Consequently, it is highly probable that, as the planet's oceans warm, the number of *Vibrio parahaemolyticus*-associated outbreaks from consuming raw oysters will rise.

Fig. 5 shows that the risk growth rate of scenario RCP8.5, relative to the time horizons, is six times higher than that of scenario RCP2.6.

The predicted risks for each season of scenario RCP8.5 were higher than those of scenario RCP2.6. For example, the risk in summer with scenario RCP8.5 was double that corresponding to winter of scenario RCP2.6. For the first 24 h postharvest, differences between the predicted risks of the two climate scenarios are observed and are higher in

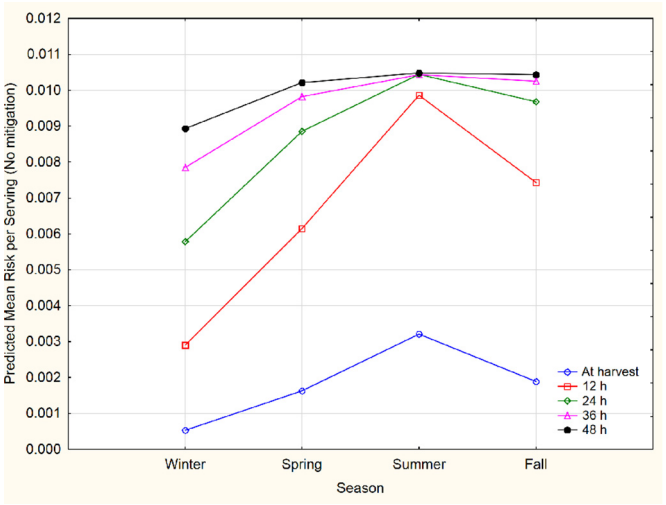

Fig. 6. Interaction season-postharvest time.

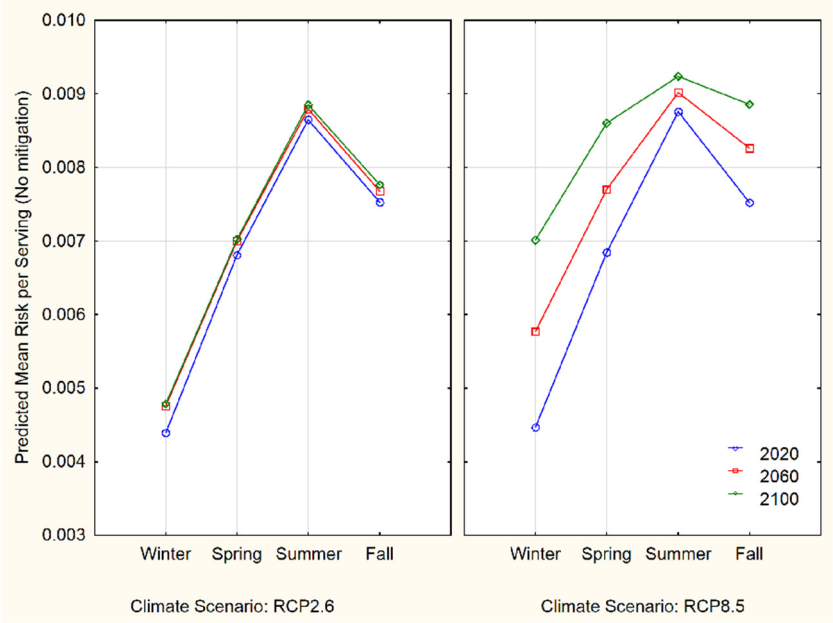

Fig. 7. Interaction season-time horizon-climate scenario.

scenario RCP8.5. However, these differences disappear after 36 h up to a plateau value of 0.10. Fig. 6 shows a summer: winter risk ratio of 6:1 at harvest, 3.3:1 at 12 h postharvest, and at 48 h postharvest no marked differences among the predicted risks of the four seasons are observed. The risk per serving of recently harvested raw oyster in Boca de Camichín during the summer under an average combination of climate scenarios and time horizons simulated in our study would be three to four times the mean risk of consuming it today on the Gulf Coast during the same season, according to the data provided by the FDA (2005) for Louisiana.

In Fig. 7, no differences are observed in predicted risks of the seasons for climate scenario RCP2.6 at the different time horizons. However, for the climate scenario RCP8.5, differences are observed among seasons and time horizons, particularly in winter, spring and, to a lesser degree, in fall. The risks in summer were not different within each climate scenario ($p = .948$).

A similar occurrence was observed with the predicted risks of postharvest times: no differences are observed among the time horizons in the climate scenario RCP2.6. However, differences were marked under the RCP8.5 climate scenario when passing from one time horizon to another.

4.2. Mitigation measures

Not all the mitigation strategies are equally effective in reducing levels of *V. parahaemolyticus* in raw oysters. Table 4 shows the characteristics and the reduction power of the mitigation strategies that were simulated.

In the upper part of Fig. 8, levels of total *V. parahaemolyticus* with no mitigation at 0 (at harvest), 12, 24 and 48 h postharvest were plotted. Twelve or more hours after harvest oysters surpass the maximum count permitted by NOM-242-SSA1 (2009) in any climate scenario or time horizon. The model predicts that, for time of harvest, some season-climate scenario-horizon combinations surpass the maximum limits of NOM-242-SSA1 (2009). In the lower part of Fig. 8 low levels of total *V. parahaemolyticus* are observed when strategies of mitigation are used. Immediate refrigeration does not bring down bacterial levels; it only maintains the level during harvest, and so another more vigorous strategy is needed to reduce levels to below that permitted by NOM-242-SSA1 (2009), particularly, in the summers of all of the climate scenarios and time horizons, in the falls with scenario RCP8.5 of the 2060 horizon and in springs with scenario RCP8.5 of the 2100 horizon. Freezing could be recommended for recently harvested oysters during all the summers with scenario RC8.5 and horizons 2060 and 2100. The model predicts that, for oysters 12 or more hours after harvest, the use of mitigation strategies that reduce at least 2-log10 microorganisms, such as the heat treatment and thermal shock, will maintain levels of total *V. parahaemolyticus* in oysters within the values permitted by NOM-242-SSA1 (2009), even under the worst climate scenario in any time horizon.

Measures for mitigating total *V. parahaemolyticus* lead to a reduction of predicted risk associated with the pathogen. Fig. 9 shows that in the measure that the global climate scenario worsens, and the time horizons occur, the levels of total *V. parahaemolyticus* in oysters with no mitigation increase, gradually increasing predicted risk. In general, using as reference the risk of becoming ill in summer from consuming recently harvested oysters with no mitigation in any climate scenario and time horizon, immediate refrigeration would reduce risk of disease by 37%. In contrast, depuration would reduce it by 94%. The more vigorous strategies—freezing, heat treatment and thermal shock would

Table 4
Mitigation strategies.

Mitigation strategy	Description	Log_{10} CFU/g Reduction
Immediate refrigeration	Harvested oysters are placed in chopped ice and, once on land, in a conventional refrigerator.	≤1
Depuration	The oysters are submerged in sea water treated with UV light to inactivate the bacteria.	0–2
Freezing	The oysters are frozen at −20 °C for 35 days	2
Thermal treatment	The oysters are heated to 50 °C for 5 min.	≥4.5
Thermal shock	The oysters are submerged in hot water (50 °C) for 5 min and cooled rapidly.	5

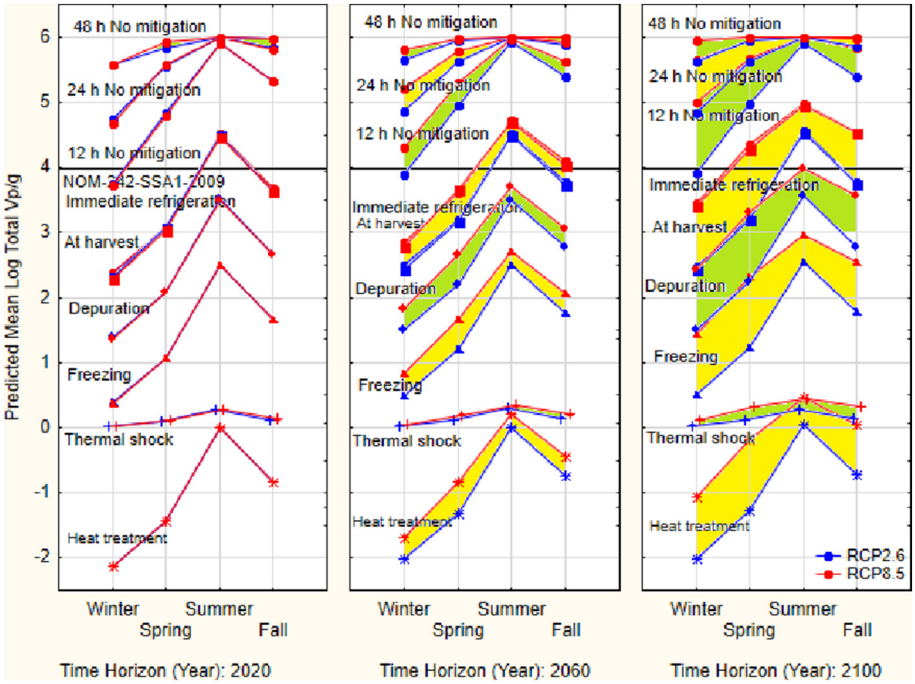

Fig. 8. Predicted levels of total *V. parahaemolyticus* per gram under mitigation strategies. Areas of the same color indicate differences in total *V. parahaemolyticus* levels between RCP2.6 and RCP 8.5 climate scenarios corresponding to a mitigation strategy or a postharvest time with no mitigation.

reduce it by almost 100% the risk of becoming ill in the summers of any climate scenario and time horizon.

These results can provide a reference point for Mexican regulating agencies to generate norms that establish sanitary specifications for raw oysters to protect the population against health risks of consuming them. Emphasis should be placed on implementing more vigorous mitigation strategies that can reduce risk of disease by almost 100%, especially during the summer months of the different combinations of climate scenarios and time horizons. In addition, this study can provide general guidelines that processors of raw oyster should satisfy to export their product to the United States and other countries.

4.3. Model validation

Levels of total and pathogenic *V. parahaemolyticus* per gram of oysters, predicted by the simulation model, were validated using the results obtained by Mendoza-Juárez (2015) from seven samples of oysters acquired in Tepic and cultivated in Boca de Camichín. This author

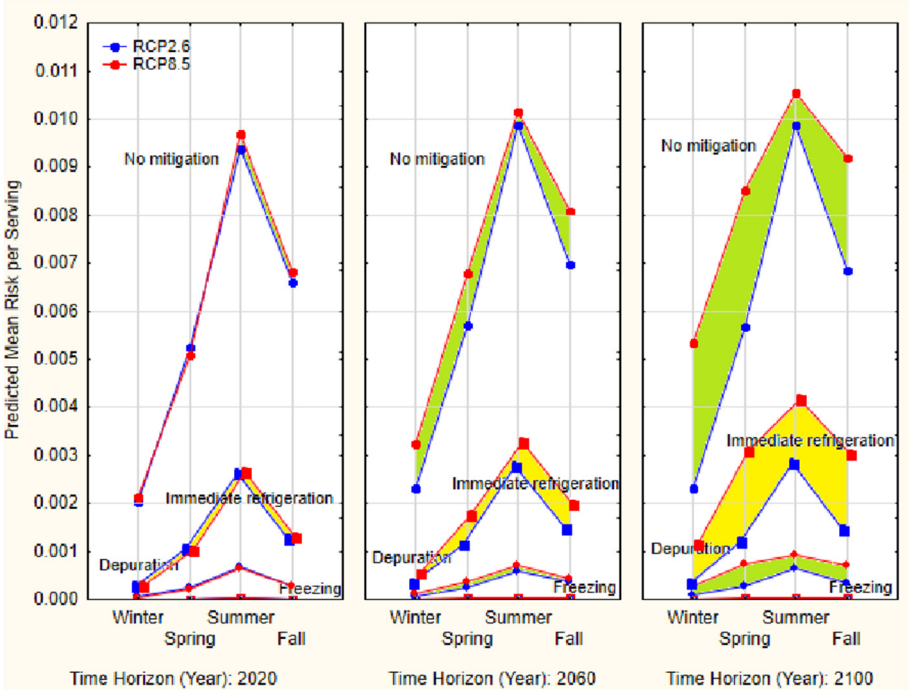

Fig. 9. Effect of mitigation on predicted risk of *V. parahaemolyticus* per serving. Areas of the same color indicate the differences in risk between the RCP2.6 and RCP 8.5 climate scenarios and correspond to a mitigation strategy.

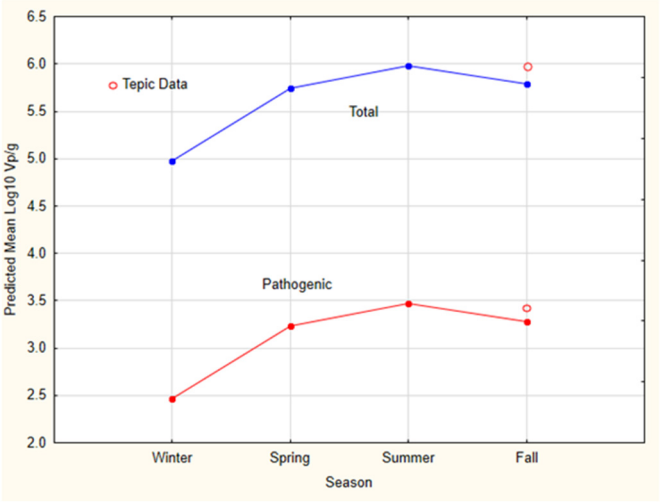

Fig. 10. Comparison of total (blue line) and pathogenic (red line) levels of *V. parahaemolyticus* predicted by the model and the values observed by Mendoza-Juárez (2015) (red circles). (For interpretation of the references to color in this figure legend, the reader is referred to the web version of this article.)

reported 3×10^3 UFC of pathogenic *V. parahaemolyticus* and 9.5×10^5 UFC of total *V. parahaemolyticus* per gram of oyster. Fig. 10 presents the levels of total and pathogenic *V. parahaemolyticus* predicted by the model for the different seasons and the data obtained by Mendoza-Juárez (2015) on September 30, 2010 (red circles). It is to be expected that there are discrepancies between the model predictions and observed values since the predicted values included the variability of many simulated years, while the observed data correspond to values obtained in a single year. However, the observed data support the validation and the predictive capability of the simulation model developed.

5. Conclusions

The evidence indicates that as the littorals warm, outbreaks of *V. parahaemolyticus* associated with consumption of raw oysters will continue to increase. At present, little is known about the impact of pathogenic *V. parahaemolyticus* on public health under different climate scenarios at different time horizons. In this study, a simulation model was developed based on the Monte Carlo method to evaluate the effect of the factors that contribute to growth of *V. parahaemolyticus* from the estuary environment up to consumption under different future climate scenarios. Moreover, the effectiveness in reducing *V. parahaemolyticus* in raw oysters by some mitigation measures was evaluated relative to the official Mexican norm NOM-242-SSA1 (2009) under different climate scenarios and time horizons. We found that the factors that most contribute to the risk of gastroenteritis are postharvest time, season, time horizon and the climate scenario. It was also made evident that the predicted risk slope of scenario RCP8.5 is six times higher than that of scenario RCP2.6, that, at the time of harvest, the risk in summer is six times higher than in the winter, and that after 48 h postharvest, the predicted risks in the four seasons are practically equal.

The model predicts that, as time horizons pass and if global warming increases, the levels of total *V. parahaemolyticus* in oyster without mitigation will gradually increase the predicted risk, and it will thus be necessary to implement mitigation strategies. Using the risk of becoming ill in summer from consuming recently harvested oysters as the reference, the simulation model predicted that immediate refrigeration will reduce the risk by 37%, depuration by 94%, and freezing, heat treatment and thermal shock will reduce the risk almost 100%, regardless of the climate scenario or the time horizon. The results of this study can provide a reference point for Mexican regulatory agencies in developing sanitary norms to protect the population against health risks caused by consumption of the mollusk. The result can also be of practical aid in implementing mitigation measures to protect consumers from *V. parahaemolyticus*. In addition, the study can provide general guidelines to raw oyster processors to enable export to the United States and other countries.

Funding

This work was supported by the Tecnológico Nacional de México (TecNM) [grant number 5411.14-P].

References

Alam, M. J., Tomochika, K. I., Miyoshi, S. I., & Shinoda, S. (2002). Environmental investigation of potentially pathogenic *Vibrio parahaemolyticus* in the Seto-Inland Sea, Japan. *FEMS Microbiology Letters, 208*, 83–87.

ANSES (2012). Agence Nationale de Sécurité Sanitaire de L'alimentation, de L'environnement et du Travail. *Data sheet on foodborne biological hazards/Vibrio parahaemolyticus*https://www.anses.fr/en/system/files/MIC2011sa0210FiEN.pdf/, Accessed date: 3 November 2017.

Baker-Austin, C., Trinanes, J. A., Taylor, N. G., Hartnell, R., Siitonen, A., & Martinez-Urtaza, J. (2013). Emerging *Vibrio* risk at high latitudes in response to ocean warming. *Nature Climate Change, 3*(1), 73–77.

Bej, A. K. (1999). Detection of total and hemolysin producing *Vibrio parahaemolyticus* in shellfish using multiplex PCR amplification of tlh, tdh, and trh. *Journal of Microbiological Methods, 36*, 215–225.

Burge, C. A., Eakin, C. M., Friedman, C. S., Froelich, B. A., Ford, S. E., Hershberger, P. K., ... Willis, B. L. (2014). Climate change influences on marine infectious diseases: Implications for management and society. *Annual Review of Marine Science, 6*, 249–277.

Cameron, A. C., & Windmeijer, F. A. G. (1996). R-squared measures for count data regression models with applications to health care utilization. *Journal of Business and Economic Statistics, 14*, 209–220.

Cameron, A. C., & Windmeijer, F. A. G. (1997). An R-squared measure of goodness of fit for some common nonlinear regression models. *Journal of Econometrics, 77*(2), 329–342.

CONAPESCA (2017). Press release. retrieved 15 December 2017 from https://www.gob.mx/conapesca/prensa/produce-nayarit-66-mil-toneladas-de-pescados-y-mariscos-se-ubica-en-el-4-lugar-nacional-por-valor-de-sus-productos.

DePaola, A., Nordstrom, J. L., Bowers, J. C., Wells, J. G., & Cook, D. W. (2003). Seasonal abundance of Total and pathogenic *Vibrio parahaemolyticus* in Alabama oysters. *Applied and Environmental Microbiology, 69*(3), 1521–1526.

FAO/WHO (2003). *Hazard characterization for pathogens in food and water: Guidelines. Microbiological Risk Assessments Series No. 3*Geneve: Food and Agriculture Organization of the United Nations/World Health Organization. 61 pp https://archive.org/details/bub_gb_7iVhBZB8jhgC/ (Accessed 3 October 2017, from) .

FAO/WHO (2011). *Risk assessment of Vibrio parahaemolyticus in seafood: Interpretative summary and Technical report. Microbiological Risk Assessment Series No. 16*Rome: Food and Agriculture Organization of the United Nations/World Health Organization. 193pp http://www.fao.org/3/a-i2225e.pdf (Accessed 7 October 2017) .

FDA (2005). Quantitative risk assessment on the public health impact of pathogenic *Vibrio parahaemolyticus* in raw oysters. https://www.fda.gov/Food/FoodScienceResearch/RiskSafetyAssessment/ucm050421.htm/ Accessed 5 September 2017.

Gkogka, E., Reij, M. W., Gorris, L. G. M., & Zwietering, M. H. (2013). The application of the appropriate level of protection (ALOP) and food safety objective (FSO) concepts in food safety management, using listeria monocytogenes in deli meats as a case study. *Food Control, 29*, 382–393.

Gooch, J. A., DePaola, A., Bowers, J., & Marshall, D. L. (2002). Growth and survival of *Vibrio parahaemolyticus* in postharvest American oysters. *Journal of Food Protection, 65*(6), 970–974.

Haas, C. N., Rose, J. B., & Gerba, C. P. (2014). *Quantitative microbial risk assessment* (2nd ed.). Wiley Blackwell.

Huang, Y.-S., Hwang, C.-A., Huang, L., Wu, V. C.-H., & Hsiao, H.-I. (2018). The risk of *Vibrio parahaemolyticus* infections associated with consumption of raw oysters as affected by processing and distribution conditions in Taiwan. *Food Control, 86*, 101–109.

INEGI (2010). *Censo Nacional de Población y Vivienda 2010.* Instituto Nacional de Estadística y Geografíahttp://www.beta.inegi.org.mx/proyectos/ccpv/2010/, Accessed date: 12 October 2017.

INEGI (2013). Fishing. Apparent and per capita consumption of fishery products, 2008 to 2013. http://www3.inegi.org.mx/sistemas/sisept/default.aspx?t=mamb349&s=est&c=35647, Accessed date: 28 October 2017.

INIFAP (2017). *Network of stations of the INIFAP. Guadalupe Victoria Station. Municipality of San Blas, Nayarit.* http://clima.inifap.gob.mx/redinifap/est.aspx?est=36178/, Accessed date: 30 October 2017.

IPCC (2014). In C. W. Team, R. K. Pachauri, & L. A. Meyer (Eds.). *Climate change 2014: Synthesis report. Contribution of Working Groups I, II and III to the fifth assessment report of the intergovernmental panel on climate change*. Geneve, Switzerland, 151 pp http://www.ipcc.ch/pdf/assessment/report/ar5/syr/SYR_AR5_FINAL_full_wcover.pdf/, Accessed date: 12 November 2017.

Iwahori, J. I., Yamamoto, A., Suzuki, H., Yamamoto, T., Tsutsui, T., Motoyama, K., et al. (2010). Quantitative risk assessment of *Vibrio parahaemolyticus* in finfish: A model of raw horse mackerel consumption in Japan. *Risk Analysis, 30*(353), 1817–1832.

Martinez-Urtaza, J., Powell, A., Jansa, J., Castro-Rey, J. L., Paz-Montero, O., García-Campello, M., ... Baker-Austin, C. (2016). Epidemiological investigation of a food-borne outbreak in Spain associated with U.S. West Coast genotypes of *Vibrio parahaemolyticus*. *Springerplus, 5*, 87.

McLaughlin, J. B., DePaola, A., Bopp, C. A., Martinek, K. A., Napolilli, N. P., Allison, C. G., ... Middaugh, J. P. (2005). Outbreak of *Vibrio parahaemolyticus* gastroenteritis associated with Alaskan oysters. *The New England Journal of Medicine, 353*(14), 1463–1470.

McMichael, A. J., & Lindgren, E. (2011). Climate change: Present and future risks to health, and necessary responses. *Journal of Internal Medicine, 270*, 401–413.

Mendoza-Juárez, L. E. (2015). *Presencia y Abundancia de Vibrios Toxigénicos en Ostiones del Género Crassostrea Comercializados en Mazatlán, Sinaloa.* (Unpublished results).

Miles, D. W., Ross, T., Olley, J., & McMeekin, T. A. (1997). Development and evaluation of a predictive model for the effect of temperature and water activity on the growth rate of *Vibrio parahaemolyticus*. *International Journal of Food Microbiology, 38*(2–3), 133–142.

Newton, A., Kendall, M., Vugia, D. J., Henao, O. L., & Mahon, B. E. (2012). Increasing rates of *Vibriosis* in the United States, 1996–2010: Review of surveillance data from 2 systems. *Clinical Infectious Diseases, 54*(0 5), S391–S395.

NOM-242-SSA1 (2009). *Productos y servicios. Productos de la pesca frescos, refrigerados, congelados y procesados. Especificaciones sanitarias y métodos de prueba.* http://www.dof.gob.mx/nota_detalle.php?codigo=5177531&fecha=10/02/2011, Accessed date: 22 October 2017.

Palisade Corportarion (2017). *@RISK (Complemento de Analisis de Riesgos para Microsoft Excel), version 7.5.2: Edicion Industrial.* Hewlett-Packard.

Pazhani, G. P., Bhowmik, S. K., Ghosh, S., Guin, S., Dutta, S., Rajendran, K., et al. (2014). Trends in the epidemiology of pandemic and non-pandemic strains of *Vibrio parahaemolyticus* isolated from diarrheal patients in Kolkata, India. *PLoS Neglected Tropical Disease, 8*(5), e2815.

Sani, A. N., Ariyawansa, S., Babji, A. S., & Hashim, J. K. (2013). The risk assessment of *Vibrio parahaemolyticus* in cooked black tiger shrimps (*Penaeus monodon*) in Malaysia. *Food Control, 31*, 546–552.

Schwarz, J. R. (2003). *Time-temperature data for rapidly chilled oysters (in ice slurry).* (Unpublished data).

Siegel, S., & Castellan, N. J. (1988). *Nonparametric statistics for the behavioral sciences* (2nd ed.). New York, NY: McGraw-Hill213–215.

Smith, B. A., Ruthman, T., Sparling, E., Auld, H., Comer, N., Young, I., ... Fazila, A. (2015). A risk modeling framework to evaluate the impacts of climate change and adaptation on food and water safety. *Food Research International, 68*, 78–85.

Sobrinho, S., Destro, M. T., Franco, B. D., & Landgraf, M. (2010). Correlation between environmental factors and prevalence of *Vibrio parahaemolyticus* in oysters harvested in the southern coastal area of Sao Paulo State, Brazil. *Applied and Environmental Microbiology, 76*, 1290–1293.

StatSoft, I. (2011). STATISTICA (data analysis software system), version 10. www.statsoft.com.

Vezzulli, L., Colwell, R. R., & Pruzzo, C. (2013). Ocean warming and spread of pathogenic *vibrios* in the aquatic environment. *Microbial Ecology, 65*(4), 817–825.

Washington State Department of Health (2000). *Vibrio monitoring data. Personal communication with Ned Therien, April 19, 2000*.

Washington State Department of Health (2001). *Vibrio monitoring data. Personal communication with Charles Kaysner, January 24, 2002*.

Yamamoto, A., Iwahori, J., Vuddhakul, V., Charernjiratragul, W., Vose, D., Osaka, K., et al. (2008). Quantitative modeling for risk assessment of *Vibrio parahaemolyticus* in bloody clams in southern Thailand. *International Journal of Food Microbiology, 124*, 70–78.